

Anisotropic *s*-wave gap and nuclear magnetic resonance in high-temperature superconductors

Asle Sudbø* and Sudip Chakravarty

Department of Physics, University of California at Los Angeles, Los Angeles, California 90024

Steven Strong and Philip W. Anderson

Department of Physics, Princeton University, Princeton, New Jersey 08544

(Received 4 November 1993)

The Knight shift and the nuclear magnetic relaxation rates W_{\perp}^{63} , W_{\parallel}^{63} , and W_{\parallel}^{17} are calculated for temperatures below the superconducting transition temperature of the high-temperature cuprate superconductors; the superscripts refer to the ^{63}Cu and the ^{17}O nuclei while the subscripts refer to the direction of the magnetic field with respect to the CuO layers. The calculations are based on a recently proposed interlayer tunneling mechanism of superconductivity in these materials. In general, the results are consistent with experiments even though the superconducting gap respects the full point-group symmetry of the lattice (anisotropic *s* wave); the anisotropy of the magnitude of the gap is an essential element.

I. INTRODUCTION

The identification of the symmetry of the superconducting order parameter is of considerable importance in constraining theories of high-temperature superconductivity. Although it is commonly agreed that the superconducting state consists of electrons paired in spin singlets, a consensus regarding the symmetry of the superconducting order parameter has not emerged.¹

Nuclear magnetic resonance (NMR) can, in principle, provide useful information regarding the wave-vector dependence of the superconducting order parameter.² One of the striking results that casts some doubt on the applicability of a BCS (Bardeen, Cooper, and Schrieffer)-type pairing theory in these materials is the absence of the Hebel-Slichter coherence peak in the NMR relaxation rates below the superconducting transition temperature, T_c .³ More recently, ^{63}Cu spin-lattice relaxation rates in $\text{YBa}_2\text{Cu}_3\text{O}_7$ (YBCO) have revealed a nonmonotonic temperature dependence of the anisotropy ratio for magnetic fields applied parallel and perpendicular to the CuO layers.⁴ The temperature dependence of the ratio of the ^{63}Cu to ^{17}O relaxation rates in parallel field appears, on the other hand, to disagree among experiments.^{3,5-7} Based on these findings, it has been argued that the superconducting state must exhibit an unconventional superconducting order parameter (i.e., an order parameter that does not respect the full point-group symmetry of the lattice) with $d_{x^2-y^2}$ symmetry, and that the *s*-wave pairing can be ruled out.⁸⁻¹⁰ In this paper, we show that this is by no means the case. The experimental observations are entirely consistent with an *s*-wave pairing and a completely gapped Fermi surface, provided that the magnitude of the gap is anisotropic. Although photoemission measurements cannot detect either the sign of the gap or nodes in the gap because of the current energy resolution, they have certainly provided evidence in favor of a gap whose magnitude varies substantially on the Fermi surface.¹¹ In a crystal, the symmetry of the gap is determined by the irreducible representations of the point

group. Thus, by an *s*-wave gap we mean a gap that transforms like the unit representation. Our conclusions are based on calculations of the Knight shift and the relaxation rates W_{\perp}^{63} , W_{\parallel}^{63} , and W_{\parallel}^{17} for the ^{63}Cu and the ^{17}O nuclei. Here the superscripts refer to the specific nucleus and the subscripts to the direction of the magnetic field with respect to the CuO layers.

II. THE MODEL

We briefly review the interlayer tunneling model that has been discussed in detail elsewhere,^{12,13} and which we use to calculate the NMR relaxation rates and the Knight shift. It consists of coupled superconducting layers where the coherent single-particle tunneling is suppressed due to the orthogonality catastrophe. In this model, the motion, even within a layer (*ab* plane), is characterized by a non-Fermi-liquid spectral function in the normal state. In contrast, we have argued that in the superconducting state the quasiparticle picture should be at least approximately valid for motion within a layer; however, the coherent motion of the quasiparticles from layer to layer is still blocked in the superconducting state. The dominant interlayer coupling is then¹²

$$H_J = - \sum_{\mathbf{k}} T_J(\mathbf{k}) [c_{\mathbf{k}\uparrow}^{(1)\dagger} c_{-\mathbf{k}\downarrow}^{(1)\dagger} c_{-\mathbf{k}\uparrow}^{(2)} c_{\mathbf{k}\uparrow}^{(2)} + \text{H.c.}] , \quad (1)$$

where $T_J(\mathbf{k}) = t_{\perp}(\mathbf{k})^2/t$, $c_{\mathbf{k}\uparrow}^{(i)\dagger}$ is an electron creation operator pertaining to the layer (*i*), of two-dimensional wave vector \mathbf{k} , and spin \uparrow . The bare matrix element determined at a high energy scale, $t_{\perp}(\mathbf{k})$, characterizes the coherent single-electron tunneling between the layers. Note that the orthogonality catastrophe does not operate at this scale. For such a bare matrix element it is adequate to use the band-structure results and parametrize $T_J(\mathbf{k})$ by $T_J(\mathbf{k}) = T_J(\cos k_x a - \cos k_y a)^4/16$,¹³ where *a* is the lattice spacing. Here, *t* is a band-structure parameter defining the motion in the *ab* plane; see below.

Thus, the Hamiltonian for a system of bilayers¹⁴ applicable to materials such as YBCO is

$$H = \sum_{\sigma, i=1,2} \varepsilon_{\mathbf{k}} c_{\mathbf{k},\sigma}^{(i)\dagger} c_{\mathbf{k},\sigma}^{(i)} + \sum_{\mathbf{k}', \mathbf{k}, i=1,2} U_{\mathbf{k}', \mathbf{k}} c_{\mathbf{k}\uparrow}^{(i)\dagger} c_{-\mathbf{k}\downarrow}^{(i)\dagger} c_{-\mathbf{k}'\downarrow}^{(i)} c_{\mathbf{k}'\uparrow}^{(i)} + H_J, \quad (2)$$

where $U_{\mathbf{k}', \mathbf{k}}$ is an in-plane pairing kernel,

$$\varepsilon_{\mathbf{k}} = -2t(\cos k_x a + \cos k_y a) + 4t' \cos k_x a \cos k_y a - \mu, \quad (3)$$

and μ is the chemical potential. This model combines the topology of the Fermi surface, observed in photoemission experiments,¹⁵ with the non-Fermi-liquid nature of the normal state.

In mean-field theory, H is diagonalized by a Bogoliubov transformation; here we assume that $b_{\mathbf{k}}^{(i)} \equiv \langle c_{-\mathbf{k}\downarrow}^{(i)} c_{\mathbf{k}\uparrow}^{(i)} \rangle$ is independent of the layer index, $b_{\mathbf{k}}^{(i)} = b_{\mathbf{k}}$. The resulting gap equation is^{12,13}

$$\Delta_{\mathbf{k}}^s [1 - T_J(\mathbf{K}) \chi_{\text{pair}}(\mathbf{k})] = \Delta_0^s \theta(\omega_D - |\varepsilon(\mathbf{k})|), \quad (4)$$

where $\Delta_{\mathbf{k}}^s \equiv \langle b_{\mathbf{k}} \rangle \chi_{\text{pair}}(\mathbf{k})$, $\chi_{\text{pair}}(\mathbf{k}) = \tanh(E_{\mathbf{k}}/2T)/2E_{\mathbf{k}}$, $E_{\mathbf{k}} = \sqrt{\varepsilon_{\mathbf{k}}^2 + (\Delta_{\mathbf{k}}^s)^2}$, and Δ_0^s is determined self-consistently from

$$\Delta_0^s = V \sum_{\mathbf{k}} \Delta_{\mathbf{k}}^s \chi_{\text{pair}}(\mathbf{k}) \theta(\omega_D - |\varepsilon_{\mathbf{k}}|). \quad (5)$$

Here, we have assumed that the in-plane attractive kernel $U_{\mathbf{k}, \mathbf{k}'}$ is due to electron-phonon interactions, and, for simplicity, have considered $U_{\mathbf{k}, \mathbf{k}'} = -V, (|\varepsilon_{\mathbf{k}}|, |\varepsilon_{\mathbf{k}'}| < \omega_D)$, where ω_D is the Debye cutoff of the in-plane phonons. The electron-phonon interaction will be parametrized by $\lambda = N(0)V$, where $N(0)$ is the density of states at the Fermi surface per spin. This choice of $U_{\mathbf{k}, \mathbf{k}'}$ leads to a natural explanation of the anomalous isotope effect observed in these materials.^{12,13} Any additional effects involving Coulomb interactions are included in the Coulomb pseudopotential parameter μ^* , as in BCS theory, or are taken into account by a simple Fermi-liquid correction. Note that Eq. (4), together with the self-consistency condition on Δ_0^s , completely determines the temperature dependence of $\Delta_{\mathbf{k}}^s(T)$.

In the superconducting state, the spin susceptibility $\chi_0(\mathbf{q}, \omega)$ is obtained from the standard BCS expression¹⁶

$$\chi_0(\mathbf{q}, \omega) = \sum_{\mathbf{k}} \left[A_{\mathbf{k}, \mathbf{q}}^+ \frac{f(E_{\mathbf{k}+\mathbf{q}}) - f(E_{\mathbf{k}})}{\omega - (E_{\mathbf{k}+\mathbf{q}} - E_{\mathbf{k}}) + i\Gamma} + \frac{1}{2} A_{\mathbf{k}, \mathbf{q}}^- \frac{1 - f(E_{\mathbf{k}+\mathbf{q}}) - f(E_{\mathbf{k}})}{\omega + (E_{\mathbf{k}+\mathbf{q}} + E_{\mathbf{k}}) + i\Gamma} + \frac{1}{2} A_{\mathbf{k}, \mathbf{q}}^- \frac{f(E_{\mathbf{k}+\mathbf{q}}) + f(E_{\mathbf{k}}) - 1}{\omega - (E_{\mathbf{k}+\mathbf{q}} + E_{\mathbf{k}}) + i\Gamma} \right], \quad (6)$$

where

$$A_{\mathbf{k}, \mathbf{q}}^{\pm} = \frac{1}{2} \left[1 \pm \frac{\varepsilon_{\mathbf{k}} \varepsilon_{\mathbf{k}+\mathbf{q}} + \Delta_{\mathbf{k}} \Delta_{\mathbf{k}+\mathbf{q}}}{E_{\mathbf{k}} E_{\mathbf{k}+\mathbf{q}}} \right], \quad (7)$$

$\Gamma = \Gamma(T)$ is the quasiparticle lifetime in the superconducting state, and $f(E_{\mathbf{k}})$ is the Fermi function. This expression is correct as long as the BCS mean-field theory is

correct. In this expression, we merely have to substitute $\Delta_{\mathbf{k}}$ by our gap $\Delta_{\mathbf{k}}^s$ that we would obtain from Eqs. (4) and (5). Strictly speaking, however, this expression is valid only in the limit $\Gamma \rightarrow 0^+$ because the quasiparticles are infinitely long lived in BCS theory. Nonetheless, this expression is often used for a finite Γ to represent possible inelastic scattering in a simple phenomenological manner. We note, however, that the justification for such a procedure to include *large* inelasticity, observed in recent experiments close to T_c ,¹⁷ is not entirely clear.

In the following, we shall extract the Knight shift and the nuclear magnetic relaxation rates from the spin susceptibility $\chi(\mathbf{q}, \omega)$, where

$$\chi(\mathbf{q}, \omega) = \frac{\chi_0(\mathbf{q}, \omega)}{1 - U \chi_0(\mathbf{q}, \omega)}. \quad (8)$$

This random-phase approximation is a simple way to incorporate the Fermi-liquid corrections in the superconducting state and is discussed in more detail below; U signifies the strength of the Fermi-liquid corrections.

A few remarks on our choice of parameters are appropriate. In our computations, we have chosen two sets of band-structure parameters t , t' , and μ in Eq. (3). For the first set,⁸ $t = 0.25$ eV, $t' = 0$, and $\mu = -0.07$ eV, corresponding to a band filling of $\langle n \rangle = 0.86$. For the second set,¹⁰ $t = 0.25$ eV, $t' = 0.45t$, and $\mu = -0.315$ eV, corresponding, again, to a band filling of $\langle n \rangle = 0.86$. We refer to the first set as set I, while the second set will be referred to as set II. The main difference is the quasiparticle motion in the ab plane. Set I produces a *closed* Fermi surface around the point Γ in the first Brillouin zone, while set II results in an *open* Fermi surface.

Because, in our theory, the critical temperature T_c of the anisotropic s -wave superconductor is rather insensitive to λ in the weak-coupling limit when $T_J(\mathbf{k})$ dominates the behavior of T_c ,^{12,13} a small variation in λ does not significantly affect the magnitude of T_c . For the bulk of the paper we have chosen, for illustrative purposes, $\lambda = 0.205$ (set I) and $\lambda = 0.225$ (set II); in addition, in order to exhibit the sensitivity of the results with respect to λ we have also computed the Knight shifts with $\lambda = 0.41$ (set I) and $\lambda = 0.45$ (set II). As in Ref. 13, we have conservatively estimated $T_J = 0.043$ eV to produce $T_c \approx 100$ K, with $\omega_D = 0.02$ eV.

To be thorough, we also include a comparison with the results obtained with an order parameter of $d_{x^2-y^2}$ symmetry, i.e.,

$$\Delta_{\mathbf{k}}^d = \frac{\Delta_0^d(T)}{2} (\cos k_x a - \cos k_y a). \quad (9)$$

For $d_{x^2-y^2}$ symmetry, we use $2\Delta_0^d/T_c = 8$, and the T dependence of $\Delta^d(T)$ has been taken to be

$$\Delta_0^d(T) = \Delta_0^d \tanh(\alpha \sqrt{T_c/T - 1}), \quad (10)$$

where $\alpha = 1.74$ reproduces the BCS-like behavior in $\Delta_0^d(T)$. As stated above, the minimum gap amplitude $\Delta_0^s(T)$ for the anisotropic s -wave pairing must be obtained self-consistently and can be tuned (effectively tuning the anisotropy of the gap) by varying λ , while maintaining T_J

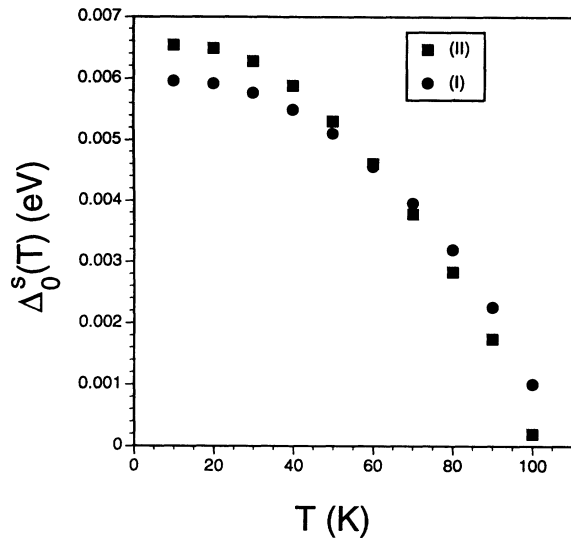


FIG. 1. Minimum values of the anisotropic *s*-wave gap $\Delta_0^s(T)$ as a function of T . The circles correspond to band-structure parameters $t=0.25$ eV, $t'=0$, $\mu=-0.07$ eV, $\langle n \rangle=0.86$ (set I), while the squares correspond to $t=0.25$ eV, $t'=0.45t$, $\mu=-0.315$ eV, $\langle n \rangle=0.86$ (set II).

constant. Note that we have used a notation where $\Delta_0^s(T)$ is the minimum of the anisotropic *s*-wave gap in contrast to $\Delta_0^d(T)$ which is the maximum of the *d*-wave gap. We apologize to our readers for any notational inconvenience.

In Fig. 1 we plot $\Delta_0^s(T)$ as a function of temperature for both sets I and II. The superconducting gap for all \mathbf{k} vanishes when $\Delta_0^s(T)$ vanishes at T_c , as can be seen from Eqs. (4) and (5). In BCS theory, with an isotropic *s*-wave gap, the temperature dependence of the gap closely approximates to its $T=0$ value at temperatures as large as $T/T_c \sim 0.7$. The modification of the temperature dependence of $\Delta_0^s(T)$ comes about as a result of the renormalization of the pair susceptibility that takes place in our theory. In effect, the replacement:

$$\chi_{\text{pair}}(\mathbf{k}) \rightarrow \frac{\chi_{\text{pair}}(\mathbf{k})}{1 - T_J(\mathbf{k})\chi_{\text{pair}}(\mathbf{k})} \quad (11)$$

when $T_J(\mathbf{k}) \neq 0$, is the reason for a non-BCS temperature dependence of $\Delta_0^s(T)$ at intermediate and higher temperatures.

III. KNIGHT SHIFT

The Knight shift is found from

$$\chi(\mathbf{q} \rightarrow 0, \omega=0) = \frac{\chi_0(0,0)}{1 - U\chi_0(0,0)}, \quad (12)$$

where $\chi_0(0,0) \equiv \chi_0(\mathbf{q} \rightarrow 0, \omega=0) = -\sum_{\mathbf{k}} \partial f(E_{\mathbf{k}}) / \partial E_{\mathbf{k}}$. The denominator accounts for the Fermi-liquid correction in the superconducting state in a simple manner. Close to T_c , there can be a high density of thermally excited quasiparticles; hence, the model of noninteracting quasiparticles cannot be valid. Following Leggett,¹⁸ one

can incorporate the Fermi-liquid corrections in the superconducting state by adding molecular fields which do not change the thermodynamics, nor any single-particle properties, but affect the low-frequency and small-wave-vector response functions. The additional molecular fields describe the distortion of the “average” Fermi surface, while the formation of Cooper pairs is not affected. There is no inconsistency in using these Fermi-liquid corrections because we have assumed that the quasiparticles in the *ab* plane are recovered in the superconducting state below T_c . In principle, for an anisotropic system, there are a large number of Fermi-liquid parameters. In practice, however, we believe that only a small number of them play any important role, because, first, the higher harmonics of the Landau functions are expected to be small, and, second, the low-order terms of the expanded Landau Hamiltonian exhaust the total number of macroscopically conserved quantities.

The Knight shifts are shown in Figs. 2 and 3. The chosen values of U are $U=0$ and $U=2t$. For the *d* wave the resulting Stoner enhancement at T_c is 1.75, while for the anisotropic *s* wave, it is 1.57, for the parameter set I. For parameter set II, they are 1.93 and 1.86, respectively. These enhancement factors are eminently reasonable.⁸⁻¹⁰ For the anisotropic *s* wave, the Knight shift at low temperatures is strongly suppressed as the electron-phonon coupling λ is increased. To better illustrate this we have also calculated the Knight shifts for $\lambda=0.41$ (set I) and $\lambda=0.45$ (set II) with all other parameters held fixed. Note that these values of λ are still within the weak-coupling regime. The results are shown in Fig. 4 and compared with the experimental results^{19,20} on YBCO for O(2,3). The results for sets I and II are essentially the same on the scale of the figure, so we show the results for only one of them, set II. The results for the Cu(2) Knight shift²¹ are similar. We caution the reader that λ is one of

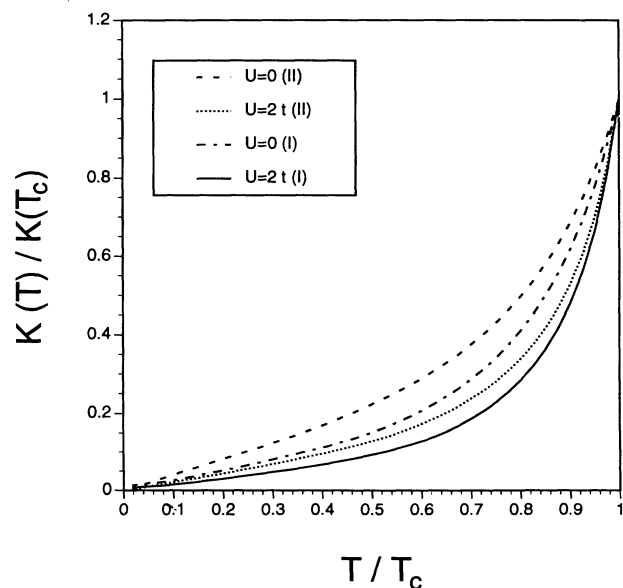


FIG. 2. Knight shift for the *d*-wave gap with $2\Delta_0^d/kT_c=8$ and band-structure parameter sets I and II as in Fig. 1.

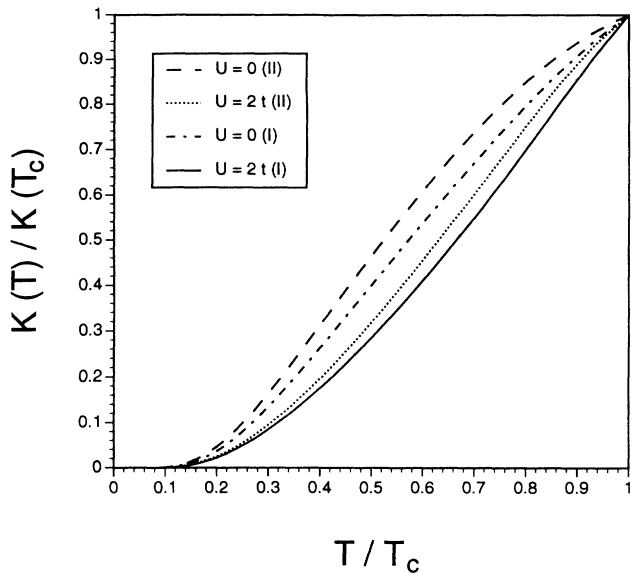


FIG. 3. Knight shift for the anisotropic s -wave gap for $\lambda=0.205$ (set I) and $\lambda=0.225$ (set II) and band-structure parameter sets I and II as in Fig. 1.

the determining parameters that controls the magnitude of the anisotropy of the gap and is expected to be different for different materials. For example, there is no reason to believe that the same parameters should apply to $\text{Bi}_2\text{Sr}_2\text{CaCu}_2\text{O}_8$ (BISCO); in fact, for this material, the Knight shift at low temperatures has a different overall temperature dependence.²²

The reader may wonder why the Knight shift at 60 K

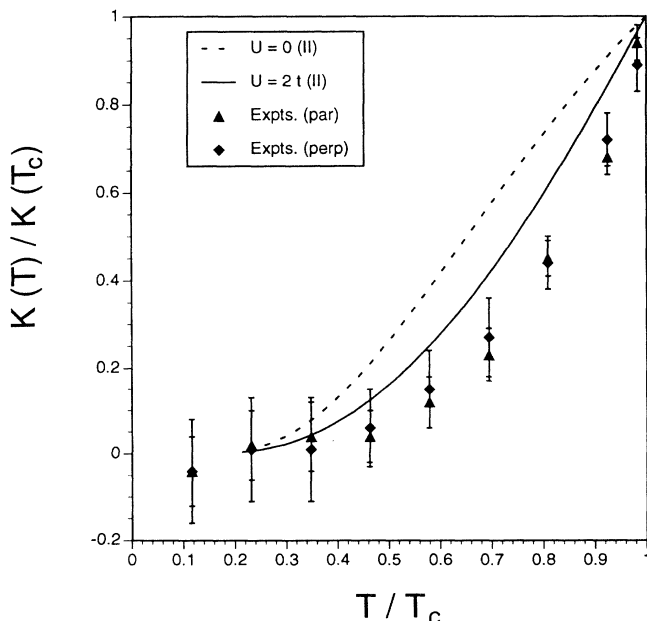


FIG. 4. Knight shift for the anisotropic s -wave gap for $\lambda=0.41$ (set I) and $\lambda=0.45$ (set II) and band-structure parameter sets I and II as in Fig. 1.

is considerable when $\Delta_0^s(T=0) \approx 70$ K. This could not possibly happen within the BCS formalism if $\Delta_0^s(T=0)$ were interpreted as the BCS gap, which it manifestly is not. This is a unique feature of our theory; while an increase in λ changes the gap anisotropy and increases the *minimum* gap $\Delta_0^s(T=0)$, it has little effect on T_c when $T_j(\mathbf{k})$ dominates in the weak-coupling limit.^{12,13} Thus, one can easily adjust $\Delta_0^s(T=0)$ to be bigger (as in BCS theory) or smaller than T_c . Suppose for the moment that the Knight shift is proportional to $e^{-\Delta_0^s(T)/T}$; then it is clear that the crossover in this exponential function, from concave to convex, takes place at temperatures $T \sim \Delta_0^s(T=0)/2$, and the shape of the curve for $T < T_c$ may appear very different for different choices of $\Delta_0^s(T=0)$ with respect to T_c . In fact, it is possible to be more quantitative if we choose the superconducting density of states to be a step function at the minimum gap edge.¹³ The logarithmic singularities at higher energies¹³ have little effect in the evaluation of the Knight shift because of the presence of the derivative of the Fermi function in the integrand. One easily finds that the Knight shift, $K(T)$, is

$$K(T) \propto \frac{1}{e^{\Delta_0^s(T)/2} + 1}. \quad (13)$$

It is possible to fit a function to $\Delta_0^s(T)$ shown in Fig. 1 and reproduce, with the help of Eq. (13), our numerically evaluated results for the Knight shift shown in Fig. 3. Finally, note that the non-BCS temperature dependence of $\Delta_0^s(T)$ also helps in producing an appreciable Knight shift for temperatures comparable to the minimum gap, as it falls more rapidly with temperature at intermediate and higher temperatures than the BCS gap, as mentioned earlier.

Note that the substantial positive curvature in the Knight shift, shown in Fig. 2, for the d wave would be absent if one were to use $2\Delta_0^d/T_c = 3.5$, which is the value one obtains self-consistently at the mean-field level. Because inelastic scattering and fluctuation effects are expected to be smaller at smaller temperatures than at T_c , they are expected to enhance the ratio $2\Delta_0^d/T_c$ from its mean-field value. This has the effect of “compressing” the Knight-shift curves along the temperature axis, introducing a stronger upward curvature consistent with experiments. The choice of large $2\Delta_0^d/T_c = 8$ for d -wave pairing can be viewed as an attempt to mimic these effects. For the case of anisotropic s -wave pairing, we have calculated the gap self-consistently within the mean-field approximation and have not taken into account the effect due to fluctuations. Although the effect of the inelastic scattering close to T_c has been incorporated in a phenomenological manner in the calculation of the relaxation rates, its effect on T_c has not been incorporated; see below. As is the case for the d wave, it is, of course, possible to adjust the parameters to improve the agreement with experiments, but this appears to be of little value.

Because the interlayer Josephson coupling in Eq. (1) is local in \mathbf{k} space, the fluctuation effects are expected to be quite important.²³ A qualitative way to understand this

effect is to consider the pseudospin formulation of the BCS theory²⁴ in which the pseudospins are situated on a continuum of \mathbf{k} points. In BCS theory each pseudospin at a given \mathbf{k} is essentially equally coupled to infinitely many pseudospins because the interaction term in the BCS reduced Hamiltonian is approximately independent of \mathbf{k} . This is why mean-field theory works so well in that case. The present problem can be viewed as two coupled systems of pseudospins, corresponding to the two individual layers, situated on two separate continua of \mathbf{k} points. The coupling between them is given by H_J in Eq. (1). In the limit that the effect of $T_J(\mathbf{k})$ dominates over that of λ , this locality in the \mathbf{k} -space coupling can lead to substantial fluctuation effects. Thus, in a more complete theory the agreement between theory and experiments close to T_c is expected to be better.

IV. RELAXATION RATES

The NMR relaxation rates, $W_{\parallel,\perp}^\alpha(T)$, are obtained from

$$W_{\parallel,\perp}^\alpha = \frac{3T}{4\mu_B^2\hbar} \lim_{\omega \rightarrow 0} \sum_{\mathbf{q}} F_{\parallel,\perp}^\alpha(\mathbf{q}) \frac{\text{Im}\chi(\mathbf{q},\omega)}{\omega}, \quad (14)$$

where μ_B is the Bohr magneton. The superscript α refer to ^{63}Cu and ^{17}O nuclei, while the subscripts \parallel and \perp indicate the direction of the applied magnetic field with respect to the CuO layers. The hyperfine form factors $F_{\parallel,\perp}^\alpha(\mathbf{q})$ are²⁵

$$\begin{aligned} F_{\perp}^{63}(\mathbf{q}) &= \frac{1}{2} [A_{\parallel} + 2B(\cos q_x a + \cos q_y a)]^2 \\ &\quad + \frac{1}{2} [A_{\perp} + 2B(\cos q_x a + \cos q_y a)]^2, \\ F_{\parallel}^{63}(\mathbf{q}) &= [A_{\perp} + 2B(\cos q_x a + \cos q_y a)]^2, \\ F_{\parallel}^{17}(\mathbf{q}) &= \frac{C^2}{2} [1 + \frac{1}{2}(\cos q_x a + \cos q_y a)]. \end{aligned} \quad (15)$$

Here, we shall use two sets of parameters, $A_{\parallel} = -4B$, $A_{\perp} = 1.60B$, $C = 0.91B$, and parameter set I,⁸ and $A_{\parallel} = -4B$, $A_{\perp} = 0.84B$, $C = 0.91B$, and parameter set II.¹⁰ Finally, we adopt $\Gamma = T_c(T/T_c)^3$ for the inelastic scattering rate and $U = 2t$ for the Fermi-liquid corrections for the *d*-wave calculations,⁸ and, somewhat inadvertently, $\Gamma = 0.8T_c(T/T_c)^3$ and $U = 2t$ for all anisotropic *s*-wave calculations. These choices for $\Gamma(T)$ incorporate, phenomenologically, the drop in the inelastic scattering rate below T_c , as observed in YBCO.¹⁷

It is appropriate to remark on the limit $\omega \rightarrow 0$ when $\Gamma(T) > 0$, in Eq. (14). Note that Eq. (8) leads to

$$\begin{aligned} \lim_{\omega \rightarrow 0} \frac{\text{Im}\chi(\mathbf{q},\omega)}{\omega} \\ = \lim_{\omega \rightarrow 0} \frac{\text{Im}\chi_0(\mathbf{q},\omega)/\omega}{[1 - U \text{Re}\chi_0(\mathbf{q},\omega)]^2 + [U \text{Im}\chi_0(\mathbf{q},\omega)]^2}, \end{aligned} \quad (16)$$

where, for $\Gamma(T) > 0$, $\lim_{\omega \rightarrow 0} \text{Im}\chi_0(\mathbf{q},\omega)/\omega \rightarrow \infty$. This problem may be circumvented in different ways. One possibility is to interpret the limit $\omega \rightarrow 0$ to mean $\omega \rightarrow \Gamma(T)$. We proceed differently and consider first $\omega \rightarrow 0$ and $\Gamma(T) = 0^+$. Then,

$$\begin{aligned} \lim_{\omega \rightarrow 0} \frac{\text{Im}\chi_0(\mathbf{q},\omega)}{\omega} = -\pi \sum_{\mathbf{k}} \left[A_{\mathbf{k},\mathbf{q}}^+ \frac{\partial f(E_{\mathbf{k}})}{\partial E_{\mathbf{k}}} \delta(E_{\mathbf{k}+\mathbf{q}} - E_{\mathbf{k}}) \right. \\ \left. + A_{\mathbf{k},\mathbf{q}}^- [1 - f(E_{\mathbf{k}+\mathbf{q}}) - f(E_{\mathbf{k}})] \right] \\ \times \delta(E_{\mathbf{k}+\mathbf{q}} + E_{\mathbf{k}}). \end{aligned} \quad (17)$$

To include lifetime effects, $\Gamma(T) > 0$, the δ functions are broadened into Lorentzians of width $\Gamma(T)$. This method has the advantage of preserving the property $\lim_{\omega \rightarrow 0} \text{Im}\chi_0(\mathbf{q},\omega) \sim \omega$. By comparing with Ref. 8, we have checked that both methods agree to within 10–20%; see below for more details. This gives us the confidence that this heuristic procedure is reasonable.

In *all* our calculations, the Hebel-Slichter peak is destroyed, due in part to the inelasticity close to T_c and in part to the strong anisotropy of the gap. At low temperatures, the \mathbf{k} sum in Eq. (17) is dominated by the minima of the excitation spectrum, $E_{\mathbf{k}}$. The temperature dependence in this regime is therefore determined by the minima of the gap, $\Delta_{\mathbf{k}}$, on the Fermi surface. Moreover, the δ function limits the \mathbf{q} sum in Eq. (14) in such a way that $E_{\mathbf{k}} = (E_{\mathbf{k}})_{\min} = E_{\mathbf{k}+\mathbf{q}}$. Therefore, when $T \ll (\Delta_{\mathbf{k}})_{\min}$, the relevant \mathbf{q} vectors connect the minima of $E_{\mathbf{k}}$ on the Fermi surface. For the Fermi surface corresponding to set I these wave vectors are close to $(0, \pi/a)$ and $(\pi/a, \pi/a)$, while for the Fermi surface corresponding to set II they are close to $(0, 0.742)\pi/a$ and $(0.742, 0.742)\pi/a$. Whether or not the gap changes sign on the Fermi surface is not qualitatively important in restricting the \mathbf{q} vectors; what is essential is that the gap be substantially anisotropic, i.e., its value at $(k_{Fx}, 0)$ must be very different from its value at (k_{Fx}, k_{Fy}) and at symmetry-related points.

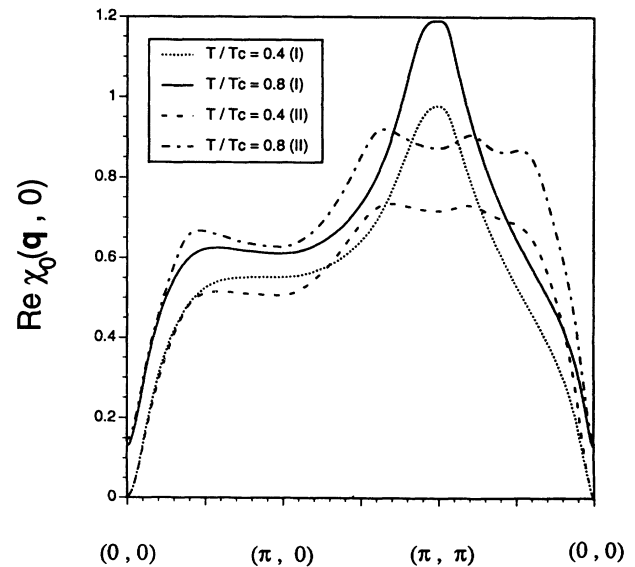


FIG. 5. $\text{Re}\chi_0(\mathbf{q},0)$ for the isotropic *s*-wave gap with $2\Delta_0/kT_c = 8$ and band-structure parameter sets I and II as in Fig. 1.

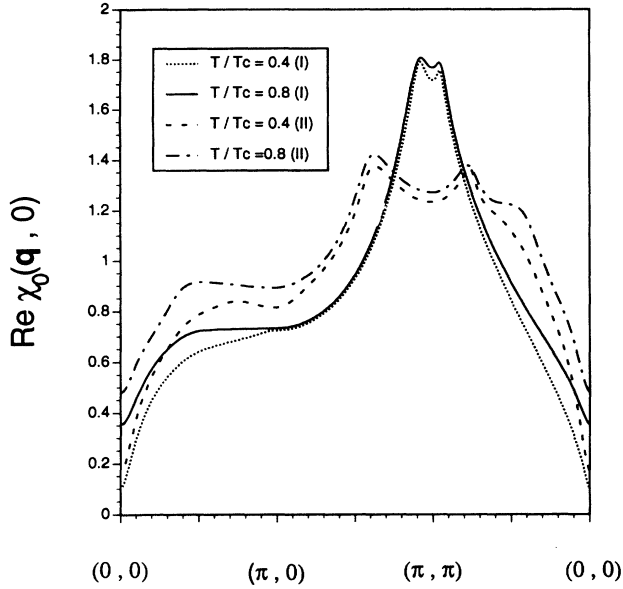


FIG. 6. $\text{Re}\chi_0(\mathbf{q}, 0)$ for the d -wave gap with $2\Delta_0^d/kT_c = 8$ and band-structure parameter sets I and II as in Fig. 1.

Consider the temperature dependence of $D_0(\mathbf{q}, T) \equiv \lim_{\omega \rightarrow 0} \text{Im}\chi_0(\mathbf{q}, \omega)/\omega$ in Eq. (14) and two representative wave vectors, $\mathbf{q}_1 = (0.05, 0)\pi/a$ and $\mathbf{q}_2 = (1.0, 0.9)\pi/a$.⁸ For all cases, isotropic s -wave pairing, d -wave pairing, and anisotropic s -wave pairing, there are remnants of upturns in $D_0(\mathbf{q}_1, T)$ just below T_c . However, for these three different types of gaps, $D_0(\mathbf{q}_2, T)$ behaves differently. The upturn for the s wave, in fact, gets sharper, while the upturn for the d wave is replaced

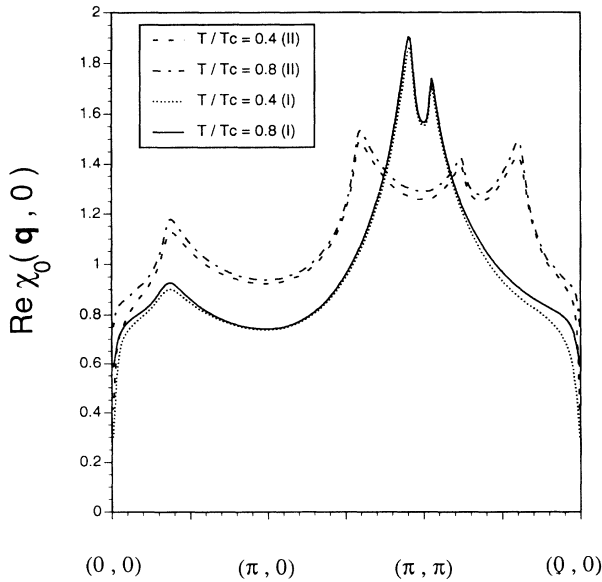


FIG. 7. $\text{Re}\chi_0(\mathbf{q}, 0)$ for the anisotropic s -wave gap with band-structure parameter sets I and II as in Fig. 1.

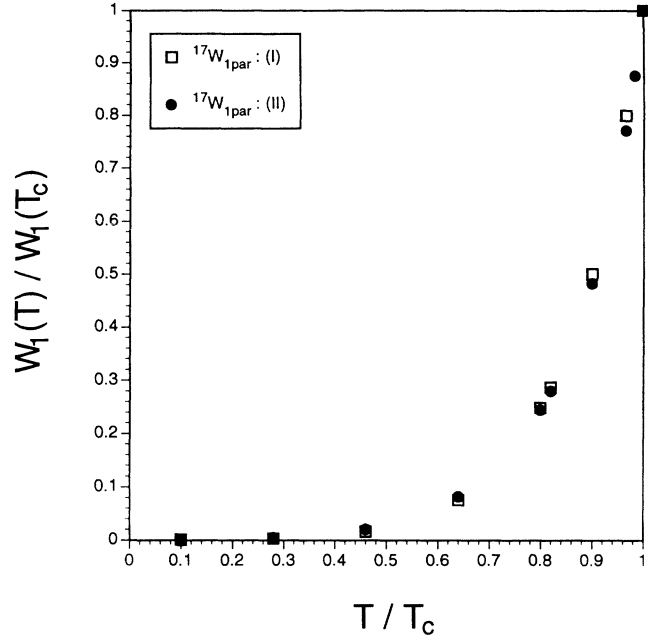


FIG. 8. Relaxation rate $W_{1\parallel}^{17}(T)/W_{1\parallel}^{17}(T_c)$ for the d -wave gap with the same parameters as in Fig. 2.

by a sharp decrease just below T_c and a considerable amount of spectral weight appears at lower temperatures. Thus, even though $D_0(\mathbf{q}, T)$ is multiplied by T and is integrated over, the d -wave relaxation rates at low temperatures are considerably enhanced over s wave. The anisotropic s -wave pairing shows a behavior intermediate between the isotropic s -wave and the d -wave pairing.

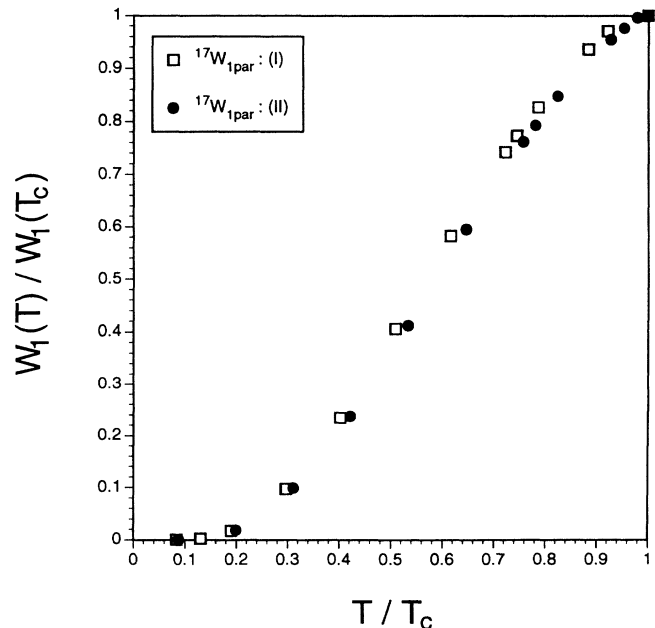


FIG. 9. Relaxation rate $W_{1\parallel}^{17}(T)/W_{1\parallel}^{17}(T_c)$ for the anisotropic s -wave gap with the same parameters as in Fig. 3.

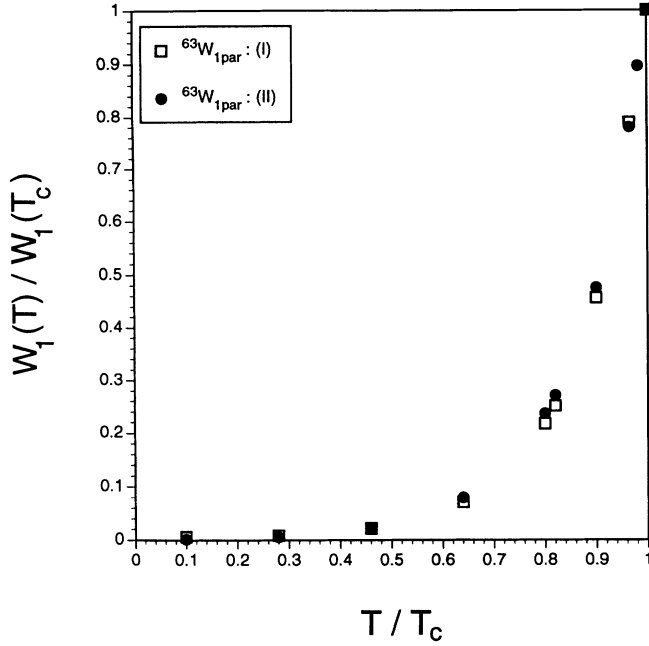


FIG. 10. Relaxation rate $W_{\parallel}^{63}(T)/W_{\parallel}^{63}(T_c)$ for the d -wave gap with the same parameters as in Fig. 2.

$D_0(\mathbf{q}_2, T)$ exhibits a slow rise just below T_c and, subsequently, does not decrease as sharply as for d -wave pairing. The slow rise below T_c , in contrast to the sharp rise in the case of the isotropic s wave, is due to the anisotropic nature of the gap, similar to the d wave. Recall that the anisotropic nature of the gap leads to a step discontinuity of the density of states at the minimum gap edge and not a square-root singularity.¹³ The absence of the

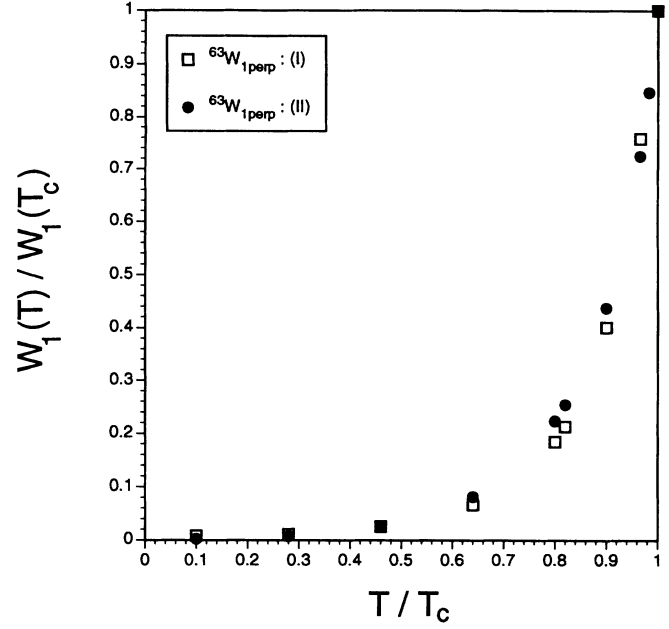


FIG. 12. Relaxation rate $W_{\parallel}^{63}(T)/W_{\parallel}^{63}(T_c)$ for the d -wave gap with the same parameters as in Fig. 2.

Hebel-Slichter peak is therefore not surprising. That $D_0(\mathbf{q}_2, T)$ does not decrease as rapidly as for the d wave is due to the different behavior of the coherence factors $A_{\mathbf{k}, \mathbf{q}}^{\pm}$. However, similar to the d wave, an appreciable amount of spectral weight appears at lower temperatures. The reasons are similar to those that led to a considerable enhancement of the Knight shift at low temperatures as compared to an isotropic s -wave gap and lead to appre-

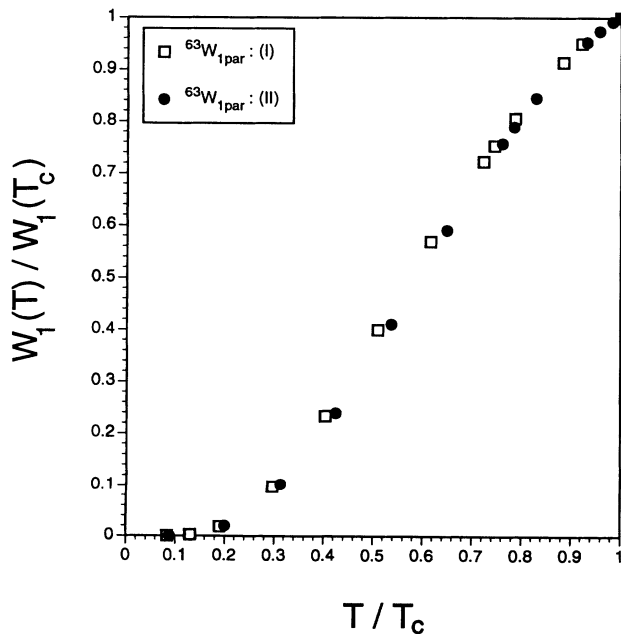


FIG. 11. Relaxation rate $W_{\parallel}^{63}(T)/W_{\parallel}^{63}(T_c)$ for the anisotropic s -wave gap with the same parameters as in Fig. 3.

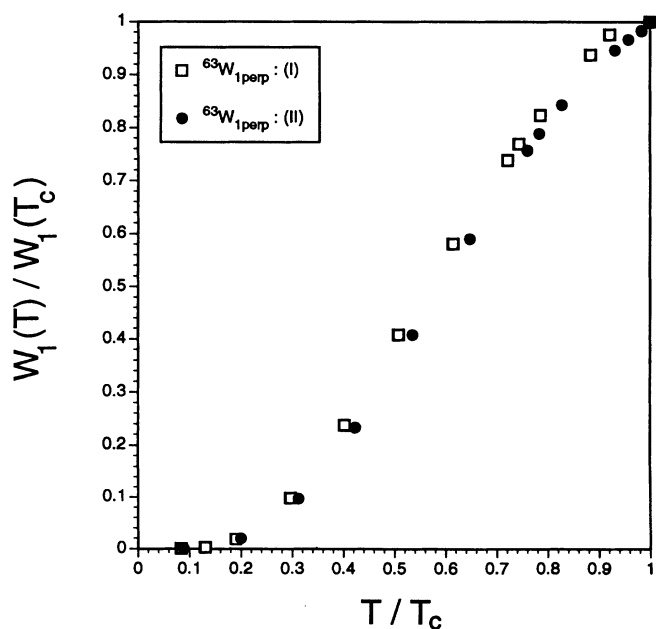


FIG. 13. Relaxation rate $W_{\parallel}^{63}(T)/W_{\parallel}^{63}(T_c)$ for the anisotropic s -wave gap with the same parameters as in Fig. 3.

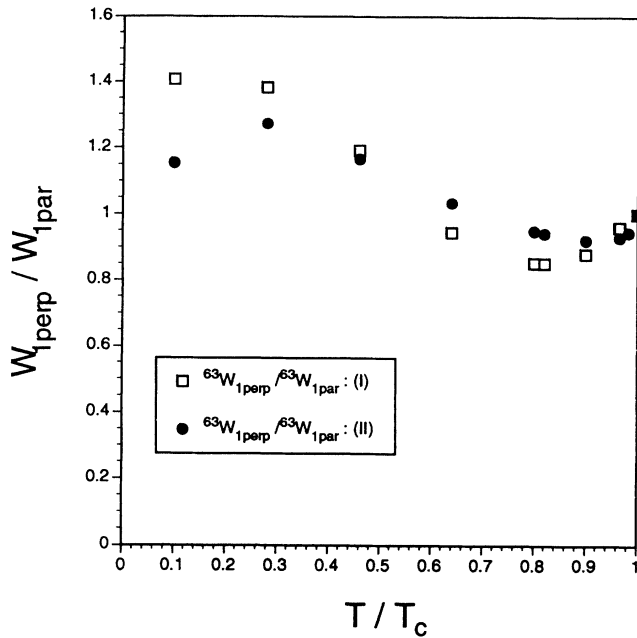


FIG. 14. Anisotropy ratio $W_{1\parallel}^{63}(T)/W_{1\parallel}^{63}(T)$ for the d -wave gap with the same parameters as in Fig. 2.

chable relaxation rates at low temperatures, in the range $\Delta_0^s/4 < T < \Delta_0^s/2$.

Consider now $\text{Re}\chi_0(\mathbf{q}, \omega)$ as a function of temperature along some typical directions in the first Brillouin zone.⁸ This quantity is shown in Figs. 5–7, at two representative temperatures, $T=0.4T_c$ and $T=0.8T_c$, for both sets of band-structure parameters, I and II. It is evident that the overall features of the \mathbf{q} dependence are dominated by the

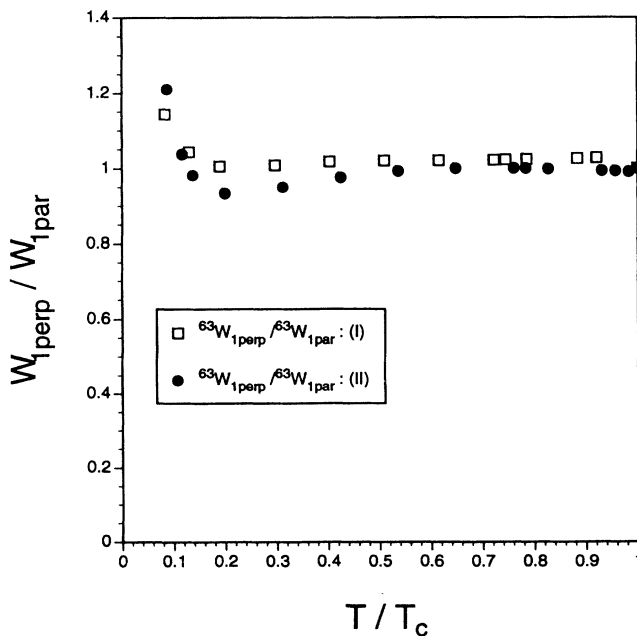


FIG. 15. Anisotropy ratio $W_{1\parallel}^{63}(T)/W_{1\parallel}^{63}(T)$ for the anisotropic s -wave gap with the same parameters as in Fig. 3.

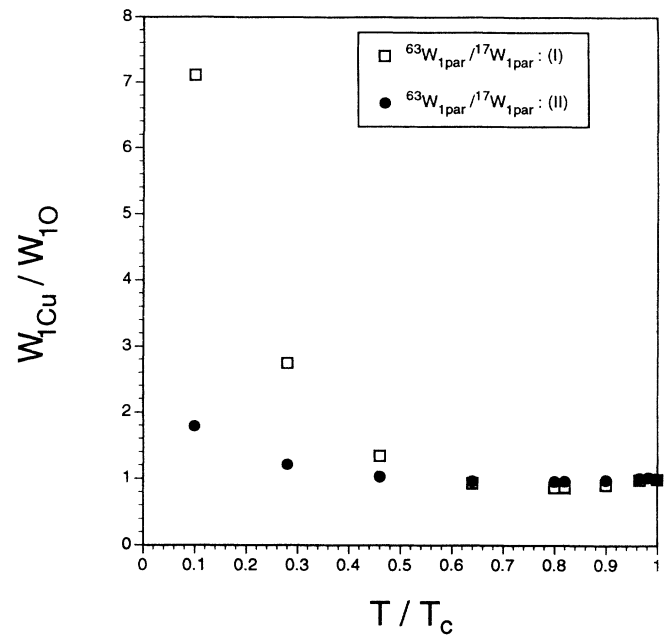


FIG. 16. Ratio of the relaxation rates $W_{1\parallel}^{63}(T)/W_{1\parallel}^{17}(T)/W_{1\parallel}^{17}(T)$ for the d -wave gap with the same parameters as in Fig. 2.

topology of the Fermi surface and not by the superconducting gap. The different gaps produce different temperature dependences, however. For both anisotropic s and d waves and for sets I and II, the temperature dependence of the peaks close to (π, π) is weak, in contrast to what one finds for an isotropic s -wave gap,⁸ at least for $T > 0.3T_c$. At higher temperatures, the minima of the anisotropic s -wave gap along the diagonals are small,

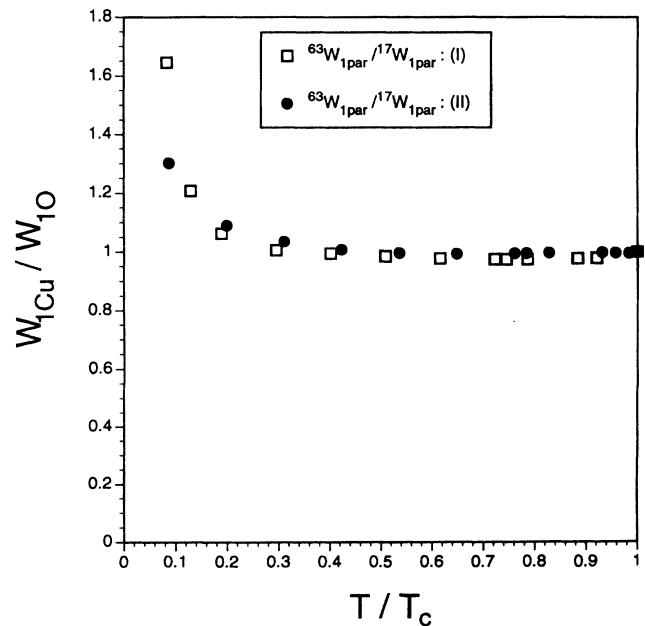


FIG. 17. Ratio of the relaxation rates $W_{1\parallel}^{63}(T)/W_{1\parallel}^{17}(T)$ for the anisotropic s -wave gap with the same parameters as in Fig. 3.

mimicking a node. For $|\mathbf{q}|\xi_{sc} < 1$, where ξ_{sc} is the superconducting coherence length, the susceptibility is suppressed at low temperatures due to the formation of singlet Cooper pairs. The suppression is stronger for the anisotropic *s* wave than the *d* wave, reflecting the activated nature of the uniform susceptibility for the anisotropic *s* wave for $T \ll T_c$. In this respect, $\text{Re}\chi_0(\mathbf{q}, 0)$ for anisotropic *s*-wave pairing appears to combine the large- \mathbf{q} behavior of a *d*-wave gap with the small- \mathbf{q} behavior of an isotropic *s*-wave gap. Because the enhancement factor in Eq. (16) is dominated by large \mathbf{q} [as seen from the $\text{Re}\chi_0(\mathbf{q}, 0)$ behavior], the temperature dependence of this factor is similar to what one would obtain for a *d*-wave gap, over a considerable range of temperature.

The relaxation rates for *d* and anisotropic *s* waves are shown in Figs. 8–13, while the anisotropy ratio, $W_{\perp}^{63}(T)/W_{\parallel}^{63}(T)$, and the Cu-to-O ratio, $W_{\perp}^{63}(T)/W_{\parallel}^{17}(T)$, are shown in Figs. 14, 15 and 16, 17 for parameter sets I and II. Similarly to the Knight shift, the upward curvature for the *d* wave is greater, although in both cases the inelastic scattering combined with the anisotropies of the gaps destroys the Hebel-Slichter coherence peak. For the anisotropic *s* wave, excellent fits to the numerical results over the entire temperature range can be obtained with the expression $W_{\perp} = (aT + bT^2 + cT^3)e^{-\Delta_0^*(0)/T}$. Of course, over a limited range of temperature it is always possible to fit a power law such as T^3 . As for the Knight shift, it is possible to adjust the parameters to make the agreement with experiments better.

It is important, however, to note that the nonmonotonic temperature dependence of the anisotropy ratio $W_{\perp}^{63}(T)/W_{\parallel}^{63}(T)$ is qualitatively reproduced even with the present set of parameters. If we keep all other parameters fixed, the shallow minimum will shift to higher temperatures if we increase the value of λ , although precise agreement with experiments⁴ on YBCO may still be difficult to achieve within the simple framework of the present paper. The experimental values of the anisotropy ratio seem to fall rather sharply at T_c and the minimum is deeper.

The temperature dependence of the Cu-to-O ratio $W_{\perp}^{63}(T)/W_{\parallel}^{17}(T)$ at low temperatures is opposite to the recent low-field measurements⁵ (see also Refs. 6 and 7),

for both *d* waves and anisotropic *s* waves; *in all cases*, the theoretical results are more in accord with the high-field results of Hammel *et al.*³ We are perplexed by this disagreement and speculate that the field inhomogeneity may be more of an issue at low fields than at high fields.

Good fits to the relaxation rates, their ratios, and the Knight shift have also been obtained assuming a gap of $s + id$ symmetry.²⁶ However, such a gap breaks time-reversal symmetry, which, at this time, can be ruled out on experimental grounds.

V. CONCLUSION

In the present paper, we have shown that it is possible to reproduce the experimental features with a reasonable set of parameters within our formalism of interlayer tunneling, but have not attempted a detailed fit to the experimental data. As was explicitly demonstrated with the Knight shifts, it is possible to adjust the parameters to further improve the agreement, but this cannot be very meaningful until we fully understand the Fermi-liquid corrections, the fluctuation effects, and the observed inelasticity close to T_c , which must await further work. We also need to understand the crossover from the non-Fermi-liquid-like spectral density to the quasiparticlelike behavior just below T_c .²⁷ Of course, if the major part of the inelasticity close to T_c is due to electron-phonon interactions, it can be incorporated by generalizing our theory^{12,13} in a manner similar to the Eliashberg formulation of conventional superconductors. This, in principle, is straightforward.

ACKNOWLEDGMENTS

We thank M. Takigawa for useful discussions and A. J. Millis for a critical reading of the manuscript. This work was supported in part by the National Science Foundation, DMR-9104873 (P.W.A. and S.S.), DMR-9220416 (S.C.), and in part by the Office of Naval Research, ONR-N00014-92-J-1101 (S.C. and A.S.). S.C. also thanks the John Simon Guggenheim Memorial Foundation for support and S.S. thanks AT&T Bell Laboratories for support.

*Permanent address: Institutt for Fysikk, Norges Tekniske Høgskole, 7034, Trondheim, Norway.

¹See, for example, B. G. Levi, *Phys. Today* **46** (5), 17 (1993), for a popular account of the current status of the field.

²For a review, see, for example, R. E. Walstedt and W. W. Warren, Jr., *Science*, **248**, 1082 (1990).

³P. C. Hammel, M. Takigawa, R. H. Heffner, Z. Fisk, and K. C. Ott, *Phys. Rev. Lett.* **63**, 1992 (1989).

⁴M. Takigawa, J. L. Smith, and W. L. Hults, *Phys. Rev. B* **44**, 7764 (1991); J. A. Martindale *et al.*, *Phys. Rev. Lett.* **68**, 702 (1992).

⁵J. A. Martindale *et al.*, *Phys. Rev. B* **47**, 9155 (1993).

⁶Y. Kohori, T. Sugata, T. Kohora, and Y. Oda, *J. Magn. Magn.*

Mater. **90-91**, 667 (1990).

⁷Y. Yoshinari, H. Yasuoka, and Y. Ueda, *J. Phys. Soc. Jpn.* **61**, 770 (1992).

⁸N. Bulut and D. J. Scalapino, *Phys. Rev. Lett.* **68**, 706 (1992); *Phys. Rev. B* **45**, 2371 (1992).

⁹J. P. Lu, *Mod. Phys. Lett. B* **6**, 547 (1992).

¹⁰D. Thelen, D. Pines, and J. P. Lu, *Phys. Rev. B* **47**, 9151 (1993).

¹¹Z.-X. Shen *et al.*, *Phys. Rev. Lett.* **70**, 1553 (1993).

¹²P. W. Anderson, in *Superconductivity, Proceedings of the ICTP Spring College in 1992*, edited by P. Butcher and Y. Lu (World Scientific, Singapore, in press).

¹³S. Chakravarty, A. Sudbø, P. W. Anderson, and S. Strong,

- Science **261**, 337 (1993); S. Chakravarty and P. W. Anderson (unpublished).
- ¹⁴For a generalization to the multilayer problem, see A. Sudbø (unpublished).
- ¹⁵For Bi-2:2:1:2, see D. S. Dessau *et al.* (unpublished); for YBCO, see J. C. Compuzano *et al.*, Phys. Rev. Lett. **64**, 2308 (1990).
- ¹⁶J. R. Schrieffer, *Superconductivity* (Benjamin/Cummings, Reading, 1983).
- ¹⁷D. A. Bonn *et al.*, Phys. Rev. Lett. **68**, 2390 (1991).
- ¹⁸A. J. Leggett, Phys. Rev. **140**, A1869 (1965); see, in particular, Sec. IV of this paper.
- ¹⁹M. Takigawa, P. C. Hammel, R. H. Heffner, Z. Fisk, K. C. Ott, and J. D. Thompson, Physica **162-164**, 853 (1989).
- ²⁰M. Takigawa, P. C. Hammel, R. H. Heffner, and Z. Fisk, Phys. Rev. B **39**, 7371 (1989).
- ²¹S. E. Barrett, D. J. Durand, C. H. Pennington, C. P. Slichter, T. A. Freedmann, J. P. Rice, and D. M. Ginsberg, Phys. Rev. B **41**, 6283 (1990).
- ²²M. Takigawa (private communication).
- ²³S. Chakravarty, G. Castilla, and A. Sudbø (unpublished).
- ²⁴P. W. Anderson, Phys. Rev. **112**, 1900 (1958).
- ²⁵F. Mila and T. M. Rice, Physica C **157**, 561 (1989).
- ²⁶Q. P. Li and R. Joynt, Phys. Rev. B **47**, 530 (1993).
- ²⁷We note here a recent paper by A. V. Balatsy, Philos. Mag. Lett. **68**, 251 (1993).